Rheumatology, 2023, **62**, 2611–2620
https://doi.org/10.1093/rheumatology/keac640
Advance access publication 18 November 2022
Original article

British Society for Rheumatology RHEUMATOLOGY OXFORD

Basic science

Rheumatoid arthritis macrophages are primed for inflammation and display bioenergetic and functional alterations

Megan M. Hanlon[1], Trudy McGarry[1,†], Viviana Marzaioli [1,†], Success Amaechi[1], Qingxuan Song[2], Sunil Nagpal[2], Douglas J. Veale[3], Ursula Fearon [1,*]

[1]Molecular Rheumatology Research Group, Trinity Biomedical Sciences Institute, Trinity College Dublin, Dublin, Ireland
[2]Immunology and Discovery Sciences, Janssen Research & Development, Philadelphia, PA, USA
[3]EULAR Centre of Excellence, Centre for Arthritis and Rheumatic Diseases, St Vincent's University Hospital, Dublin, Ireland

*Correspondence to: Ursula Fearon, Molecular Rheumatology Research Group, School of Medicine, Trinity Biomedical Sciences Institute, 152-160 Pearse Street, Trinity College Dublin D02 R590, Dublin, Ireland. E-mail: fearonu@tcd.ie

†Trudy McGarry and Viviana Marzaioli contributed equally to this study.

Abstract

Objectives: Myeloid cells with a monocyte/macrophage phenotype are present in large numbers in the RA joint, significantly contributing to disease; however, distinct macrophage functions have yet to be elucidated. This study investigates the metabolic activity of infiltrating polarized macrophages and their impact on pro-inflammatory responses in RA.

Methods: $CD14^+$ monocytes from RA and healthy control (HC) bloods were isolated and examined *ex vivo* or following differentiation into 'M1/M2' macrophages. Inflammatory responses and metabolic analysis ± specific inhibitors were quantified by RT-PCR, western blot, Seahorse XFe technology, phagocytosis assays and transmission electron microscopy along with RNA-sequencing (RNA-seq) transcriptomic analysis.

Results: Circulating RA monocytes are hyper-inflammatory upon stimulation, with significantly higher expression of key cytokines compared with HC ($P < 0.05$) a phenotype which is maintained upon differentiation into mature *ex vivo* polarized macrophages. This induction in pro-inflammatory mechanisms is paralleled by cellular bioenergetic changes. RA macrophages are highly metabolic, with a robust boost in both oxidative phosphorylation and glycolysis in RA along with altered mitochondrial morphology compared with HC. RNA-seq analysis revealed divergent transcriptional variance between pro- and anti-inflammatory RA macrophages, revealing a role for STAT3 and NAMPT in driving macrophage activation states. STAT3

Graphical Abstract

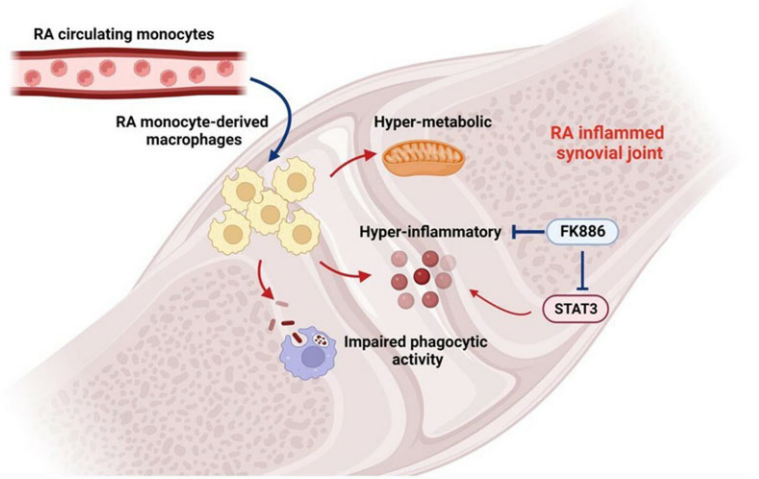

Circulating $CD14^+$ monocytes enter the inflamed RA synovium and differentiate into monocyte-derived macrophages. These macrophages clearly memorise the phenotype of their circulating precursor cells and display hyper-inflammatory and hyper-metabolic profiles. Interestingly inflammatory macrophages also display impaired phagocytic activity. Inhibition of novel metabolic cofactor NAMPT reverses this phenotype and restores macrophage homeostasis in part due to reciprocal inhibition of STAT3 activation. Created using Biorender.com.

Received: 17 June 2022. **Accepted:** 28 October 2022

and NAMPT inhibition results in significant decrease in pro-inflammatory gene expression observed in RA macrophages. Interestingly, NAMPT inhibition specifically restores macrophage phagocytic function and results in reciprocal STAT3 inhibition, linking these two signalling pathways.

Conclusion: This study demonstrates a unique inflammatory and metabolic phenotype of RA monocyte-derived macrophages and identifies a key role for NAMPT and STAT3 signalling in regulating this phenotype.

Keywords: macrophage, RA, bioenergetics, monocyte, STAT3, NAMPT

Rheumatology key messages

- RA macrophages clearly memorize the phenotype of their precursor cells and are primed for inflammation.
- RA-activated macrophages display a hyper-inflammatory and hyper-metabolic phenotype coupled with blunted phagocytosis.
- NAMPT and STAT3 regulate this distinct phenotype; manipulation of these pathways restores macrophage homeostatic functions.

Introduction

Myeloid cells such as macrophages and monocytes make up the majority of innate immune cells during inflammation and are believed to be local and systemic amplifiers of disease critically involved in shaping inflammation through a variety of mechanisms. Notably, activated macrophages promote a number of pro-inflammatory mechanisms in the synovium such as abundant overexpression of crucial RA-associated cytokines such as TNFα and IL-1β [1]. In addition, macrophages secrete high levels of matrix-degrading enzymes, present antigen to T and B cells, phagocytose and drive bone resorption [2–4]. Furthermore, $CD68^+$ synovial macrophage expression strongly correlates with disease activity and is inversely related to *in vivo* synovial PO_2 levels [5–7], and synovial sub-lining (SL) macrophages are the only cell type found to date that are consistently reduced in RA responders, regardless of treatment type [5, 8–11].

Upon entry into the synovium, monocytes differentiate into macrophages in response to factors such as M-CSF (CSF1), IL-34 or GM-CSF (CSF2), inducing the expression of macrophage-associated genes [12]. This process is particularly enhanced in response to inflammatory conditions and physiological stress [13]. Typically, macrophage functional subsets have been characterized into classical inflammatory 'M1-like' and tissue-resolving 'M2-like' phenotypes. The 'M1-like' macrophages are described as the dominant phenotype in the RA joint. Möttönen and colleagues demonstrated that 68% of RA SF macrophage-like synoviocytes display a phenotype typical of inflammatory macrophages [14]. A more recent study confirmed the pro-inflammatory phenotype of *ex vivo* isolated $CD14^+$ RA SF macrophages [15]. This is perhaps due to the inflammatory milieu of the synovial microenvironment [16].

The differing functions of polarized macrophages may be influenced by their bioenergetic status, as recent studies have indicated enhanced glycolytic flux and a concomitant impairment in the tricarboxylic acid (TCA) cycle is associated with the inflammatory function of 'M1-like' macrophages [17]. This is particularly interesting in the context of RA whereby synovial $CD68^+$ macrophages are strongly associated with metabolic activity, mitochondrial dysfunction and oxidative stress *in vivo*, and inversely related to *in vivo* synovial pO_2 levels [5, 7, 8, 16].

We have previously reported that circulating monocytes in RA are primed for hyper-inflammatory and hyper-metabolic mechanisms, an early phenomenon that precedes clinical manifestations of disease [18]. Therefore, in this study we investigate whether this distinct phenotype is maintained in RA myeloid cells upon differentiation into mature *ex vivo* macrophages and whether we can identify potential targets for resolution of inflammation.

Patients and methods

Extended methods are available in Supplementary Data S1, available at *Rheumatology* online.

Patient recruitment

Patients with established RA were recruited from the Rheumatology Department at St Vincent's University Hospital, Dublin, Ireland; patient demographics are shown in Table 1. Patients fulfilling the ACR classification criteria were included in this investigation [19]; all patients were required to give fully informed written consent, approved by the St Vincent's Healthcare Group Medical Research and Ethics Committee. Patient assessment included same-day tender and swollen joint count (TJC/SJC), ESR, CRP, RF and ACPA, and global health visual analogue scale [19]. Healthy blood was obtained from anonymous healthy control (HC) donors from St James's Hospital, Dublin. Ethical approval was obtained by the School of Medicine Research Ethics Committee, Trinity College Dublin.

$CD14^+$ monocyte and monocyte-derived macrophage isolation and culture

Peripheral blood mononuclear cells (PBMC) were isolated from blood by density gradient centrifugation (Lymphoprep; Stemcell Technologies, Vancouver, Canada). A positive selection of

Table 1. Patient demographics

Characteristic	Mean	Percentage or range
Age, years	55.4	24–88
Gender, female, *n*	28	62
RF positive, *n*	26	58
ACPA positive, *n*	25	55.5
Disease duration, years	11.84	<1–45
DAS28, *n*	3.15	1.24–6.64
CRP, *n*	7.4	<1–32.3
On MTX, *n*	15	33.33
Treatment naïve, *n*	13	29
On NSAIDs, *n*	4	8.90
On biologic, *n*	9	20
On DMARD, *n*	4	8.90

Patient characteristics for isolated monocytes from RA blood ($n = 45$). Values reflect either the group average or the range in each group with given criteria.

$CD14^+$ cells was performed by adding MACS superparamagnetic microbeads (Miltenyi-Biotec, Bergisch Gladbach, Germany) conjugated with monoclonal anti-human CD14 antibodies to freshly prepared PBMC in MACS buffer (Miltenyi-Biotec). Isolated PBMC were then magnetically sorted and labelled to yield a pure (≥95%) population of $CD14^+$ monocytes. Freshly isolated monocytes were cultured in RPMI 1640 (Thermo Fisher Scientific, MA, USA) supplemented with 10% fetal calf serum, HEPES (20 mM), penicillin–streptomycin (100 μg/ml), amphotericin B (0.25 μg/ml) (Gibco-BRL, UK) and 50 μg/ml of gentamycin (Sigma-Aldrich, Missouri, USA).

$CD14^+$ monocytes were seeded at a density of 2×10^6 cells/well in a 6-well plate and cultured in complete RPMI supplemented with M-CSF (50 ng/ml) (PeproTech, London, UK) for 8 days to derive *in vitro* macrophage cultures. Macrophages were then polarized for 24 h to either 'M1-like' macrophages using LPS (100 ng/ml) (Enzo Life Sciences, Belgium) or IFNγ (20 ng/ml) (PeproTech, UK) or 'M2-like' macrophages using IL-4 (20 ng/ml) (PeproTech, UK). For functional studies, macrophages were detached using Accutase cell detachment solution (Sigma-Aldrich, Ireland) for 20 min at 37°C. M1-polarized macrophages were also inhibited with STATTIC (5 μM) and FK866 (100 μM) for 24 h following polarization. $CD14^+$ monocytes were also analysed either *ex vivo* or following 24 h stimulations with LPS (100 ng/ml) (Enzo Life Science, UK).

Seahorse

Oxygen consumption rate (OCR) and extracellular acidification rate (ECAR), reflecting oxidative phosphorylation and glycolysis respectively, were measured using the Seahorse XFe96 analyser (Agilent Technologies). Macrophages were detached using Accutase cell-detachment solution (Sigma-Aldrich, Ireland), seeded at a density of 50 000 cells/well in a 96-well Seahorse microplate (Agilent Technologies) and allowed to adhere for 1 h in RPMI. Cells were polarized into 'M1-like' and 'M2-like' macrophages and incubated overnight. Cells were then washed and further incubated with Seahorse medium for 1 h at 37°C in a non-CO_2 incubator, before undergoing a Mito Stress test using the Seahorse XFe96 Analyser. Basal oxidative phosphorylation/glycolysis was calculated by the average of three baseline OCR/ECAR measurements, respectively. Specific metabolic inhibitors: oligomycin (2 μg/ml), trifluorocarbonylcyanide phenylhydrazone (FCCP) (mitochondrial uncoupler) (5 μM) and antimycin A (complex-III inhibitor) (2 μM) (all Agilent Technologies) were further injected to assess the metabolic capacity of macrophages.

Transmission electron microscopy

To investigate the morphology and number of mitochondria in RA and HC monocyte–derived macrophages, transmission electron microscopy was used. Macrophages were seeded at density of 2×10^6 cells/well on day 0 and polarized on day 8 for 24 h. Cells were fixed in glutaraldehyde (3% in 0.05 M potassium phosphate buffer, pH 6.8; Sigma-Aldrich) for 1 h at room temperature. Samples were processed and analysed using a Jeol-JEM2100 LaB6 (operated at 100 Kv). Digital images were obtained using an AMT XR80 capture system and ImageJ software. High-powered images of 5 cells/sample were taken. The number of mitochondria was counted and the average, per sample, was calculated. The average number of elongated mitochondria/field of view from $n = 5$ samples were also counted and represented as a percentage of total mitochondria (elongated and regular oval shaped).

Phagocytosis assay

Receptor-mediated endocytosis was assessed using DQ-labelled OVA (Thermo Fisher Scientific, MA, USA). Macrophages were detached using Accutase, washed, collected in flow tubes and incubated with 4 μL OVA-DQ either at 0°C (passive phagocytosis) or 37°C (active phagocytosis) for 15 min, and subsequently washed twice. Quantification of the cells' phagocytic profiles was obtained using FortessaFlow-Cytometer and analysed using FlowJo software.

RNA-sequencing

High quality RNA was isolated from RA polarized monocyte-derived macrophages using the RNeasy kit (QIAGEN) and the purity of RNA samples was assessed using a NanoDrop 2000 spectrophotometer (ThermoFisher). RNA samples were reverse transcribed and sequence libraries were generated by Janssen Pharmaceutical (Spring House, PA, USA) using the NuGen Ovation Universal RNA-sequencing (RNA-seq) System. The resulting sequencing libraries were analysed using the Cali-per LabChip GX and quantified using KAPA qPCR. Libraries were normalized and pooled. Each pool was then clustered and sequenced on an Illumina NextSeq500 instrument using 2× 100 bp paired-end reads, following manufacturer's instructions. Raw read quality was evaluated using FastQC before reads were trimmed for adaptors and sequence quality. Trimmed reads were aligned to human CRCh38.84 reference genome using STAR RNA-seq aligner. Aligned reads were quantified for each gene. Aligned data were evaluated for quality using several quality metrics (e.g. mapping rate, coverage) and visually inspected for samples deviating from the population across multiple metrics and principal component analysis. Statistical analysis of RNA-seq data was performed in R (version-3.5.1).

Differential gene analysis was performed with edgeR package to normalize and identify differentially expressed genes (DEGs) from counts data. Gene counts were converted to $\log_2$ counts per million, quantile normalized, and precision weighted. RNA-seq gene features were considered differentially expressed if they satisfied a 2-fold change and false discovery rate <0.05 cut-off. False discovery rate control was performed with the Benjamini–Hochberg procedure. Heatmaps and volcano plots were generated in R with the heatmap.2 and EnhancedVolcano functions in the gplots package. Hierarchical clustering was performed with Ward's linkage. Ingenuity Pathway Analysis (IPA) was used to identify canonical pathways overrepresented within DEGs.

Results

Inflammatory profiling of RA circulating monocyte and monocyte-derived macrophages

To examine the role of myeloid cells in the pathogenesis of RA, we examined the frequencies of circulating monocyte populations in healthy and RA peripheral blood. A significant decrease in frequency of classical monocytes coupled with a significant increase intermediate monocytes (Fig. 1A, $P < 0.05$) was demonstrated in RA compared with HC, with little difference observed for the non-classical subset (Fig. 1A).

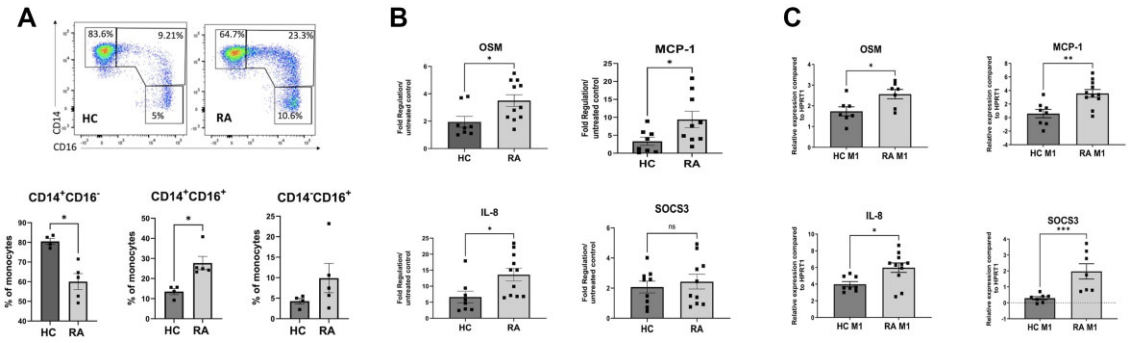

Figure 1. RA myeloid cells are hyper-inflammatory. (**A**) Representative flow cytometry plots and dot plots depicting frequency of monocyte subsets in RA ($n = 4$) and HC blood ($n = 4$). Data expressed as mean (S.E.M.) using Mann–Whitney U test; $^*P < 0.05$ significantly different from healthy. (**B**) Dot plots of inflammatory gene expression in RA ($n = 10$–11) and HC ($n = 8$–9) activated circulating monocytes. (**C**) Dot plots of inflammatory gene expression in RA ($n = 7$–11) and HC ($n = 7$–8) monocyte-derived 'M1' macrophages. Data normalized to housekeeping control, expressed as mean (S.E.M.) using unpaired t-test or Mann–Whitney U test; $^*P < 0.05$ significantly different from HC. HC: healthy control

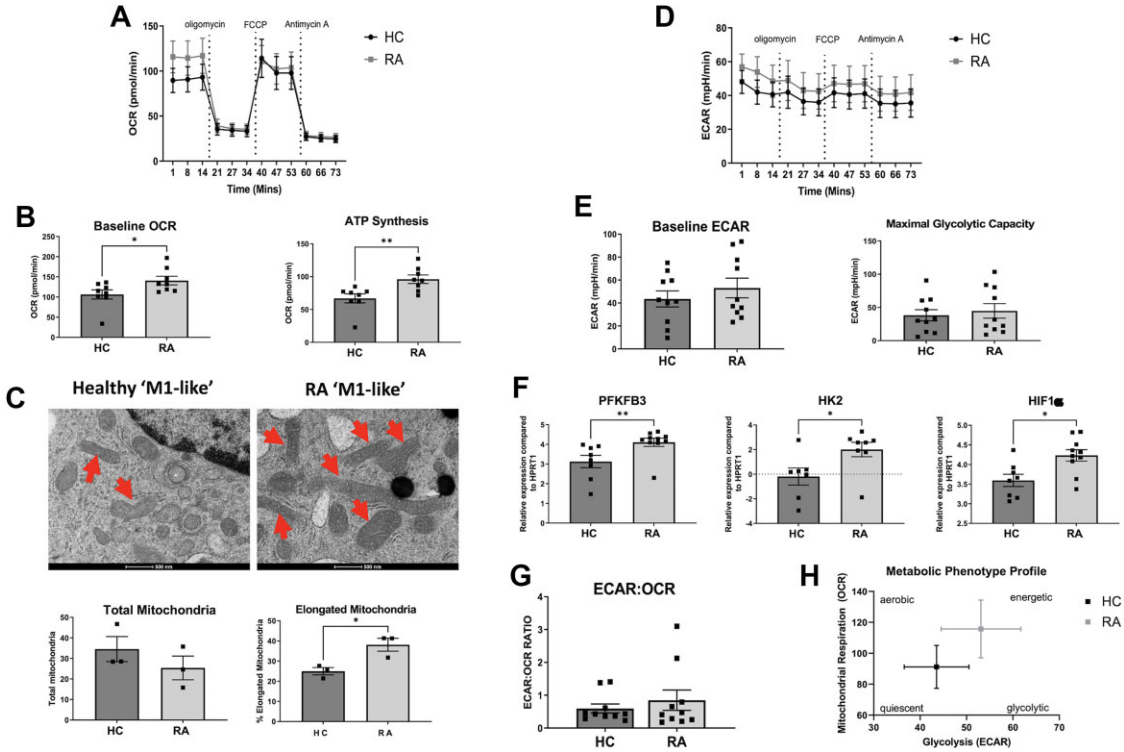

Figure 2. RA monocyte-derived macrophages have altered cellular bioenergetics. (**A**) Average OCR seahorse profile of HC ($n = 10$) and RA ($n = 10$) M1 macrophages before and after injections of oligomycin, FCCP and antimycin (**B**) Graphs demonstrating baseline OCR and ATP synthesis quantification of HC ($n = 10$) and RA ($n = 10$) M1 macrophages. (**C**) Representative transmission electron microscopy images of RA and HC M1 macrophages. Dense, elongated mitochondria are indicated by red arrows. Scale bar represents 500 nm. Graphs represent total numbers of mitochondria, and percentage of elongated mitochondria in HC ($n = 3$) and RA ($n = 3$) M1 macrophages. (**D**) Average ECAR profile and (**E**) dot plots representing baseline ECAR and maximal glycolytic capacity of HC ($n = 10$) and RA ($n = 10$) M1 macrophages. (**F**) Dot plots depicting gene expression of *PFKFB3*, *HK2* and *HIF1α* in RA ($n = 8$–10) and HC ($n = 7$–8). (**G**) Overall metabolic profile of HC ($n = 10$) and RA ($n = 10$) monocyte-derived M1 macrophages. Data expressed as mean (S.E.M.) and using Mann–Whitney U test or unpaired t-test; $^*P < 0.05$, $^{**}P < 0.01$, significantly different from HC. OCR: oxygen consumption rate; FCCP: trifluorocarbonylcyanide phenylhydrazone; ECAR: extracellular acidification rate; HC: healthy control

Next, we focused on the entire CD14$^+$ monocyte population, reflective of both classical and intermediate subsets (Supplementary Fig. S1, available at *Rheumatology* online) and examined inflammatory gene expression. We demonstrated that CD14$^+$ RA monocytes are primed for inflammatory mechanisms with significant increases in pro-inflammatory cytokines such as OSM, MCP-1 and IL-8 (Fig. 1B, $P < 0.05$) compared with HC.

To assess whether the hyper-inflammatory phenotype of monocytes is maintained upon differentiation into macrophages, we cultured monocytes for 8 days in the presences of M-CSF to generate monocyte-derived macrophages. We demonstrated that mature *ex vivo* RA macrophages clearly memorize the inflammatory phenotype of their precursor cells as indicated by significant increases in inflammatory markers in RA macrophages compared with HC (Fig. 1C, $P < 0.05$). Together these data indicate that monocytes in the RA periphery are pre-programmed for inflammation and upon differentiation into macrophages at the site of inflammation, this memory bias towards inflammation persists.

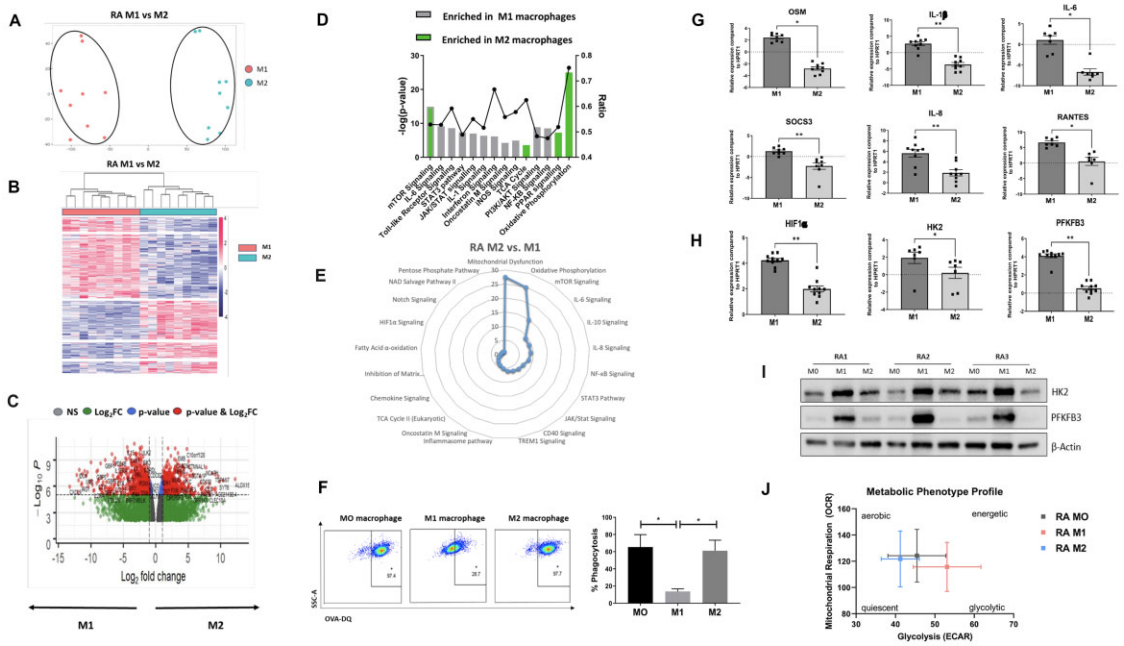

Figure 3. RA monocyte-derived macrophages are transcriptionally and functionally distinct. (**A**) Principal component analysis, (**B**) unsupervised hierarchical clustered heatmap and (**C**) volcano plot of DEGs between in RA M1 and M2 monocyte-derived macrophages. (**D**) Ingenuity Pathway Analysis of enriched pathways in RA M1 compared with M2. (**E**) Dot plots depicting inflammatory and metabolic gene expression of RA polarized monocyte-derived macrophages ($n = 7$–10). (**F**) Representative western blot demonstrating protein expression of HK2, PFKFB3 and β-actin for RA M0, M1 and M2 macrophages from three independent RA patients. (**G**) Overall metabolic profiles of polarized RA M0, M1 and M2 macrophages ($n = 10$). (**H**) Representative flow cytometry dot plots demonstrating the phagocytic capacity of RA M0, M1 and M2 macrophages. (**I**) Bar graph representing the difference in phagocytic ability between M0, M1 and M2 macrophages ($n = 10$). Data expressed as mean (S.E.M.) using Wilcoxon signed rank and paired *t*-test; $^*P < 0.05$ significantly different. DEGs: differentially expressed genes

RA macrophages are highly metabolically active

Using the Seahorse XFe96 Flux analyser we examined the bioenergetic profiles of RA and HC monocyte-derived macrophages. Average OCR indicates a significant induction of baseline OCR and hence, an increased reliance on oxidative phosphorylation in RA 'M1-like' macrophages compared with their healthy counterparts (Fig. 2A and B, $P < 0.05$). This is paralleled by a significant induction of ATP synthesis in RA 'M1-like' compared with HC 'M1-like' (Fig. 2B, $P < 0.05$). While ultrastructural analysis demonstrated similar numbers of mitochondria between RA and HC macrophages (Fig. 2C), examination of mitochondrial morphology revealed that RA macrophages displayed a greater frequency of larger, more dense, elongated mitochondria (red arrows) (Fig. 2C, $P < 0.05$), suggesting alterations in mitochondrial function.

Moreover, average ECAR profiles demonstrate a trending increase in baseline glycolysis in RA macrophages compared with HC (Fig. 2D and E). This was associated with increased maximal glycolytic capacity and significantly increased expression of key metabolic genes, *PFKFB3*, *HK2* and *HIF1α*, in RA macrophages compared with HC (Fig. 2E and F, $P < 0.05$). This resulted in an overall metabolic shift in the phenotypic profile whereby RA macrophages are in a highly energetic phenotype compared with HC (Fig. 2G).

Transcriptional profiling of RA polarized macrophages

Next RNA-seq analysis was performed on 'M1-like' and 'M2-like' macrophages. Principal component analysis, unsupervised hierarchical clustering and volcano plots demonstrate that RA 'M1-like' macrophages cluster separately from 'M2-like' (Fig. 3A–C), indicating distinct transcriptional signatures. IPA revealed enrichment of many key inflammatory and metabolic pathways as demonstrated in Fig. 3D. We then performed *in vitro* analysis of polarized RA macrophages to further validate transcriptional data. Firstly, we demonstrate significant enrichment of *OSM*, *IL-6*, *IL-1* and chemokines (*RANTES*) in RA 'M1-like' macrophages compared with 'M2-like' (Fig. 3G). Moreover, IPA analysis revealed enrichment of metabolic pathways such as HIF1α signalling in 'M1-like' macrophages. We further validated the enrichment of *HIF1α* and other key glycolytic enzymes, *HK2* and *PFKFB3*, at both the gene and protein level in RA inflammatory macrophages (Fig. 3H and I). In contrast, TCA cycle and oxidative phosphorylation pathways were observed to be key pathways in anti-inflammatory macrophages (Fig. 3D and E). Using the Seahorse analyser, we demonstrate that RA 'M2-like' macrophages are in an aerobic state while pro-inflammatory 'M1-like' have transitioned to a glycolytic/energetic phenotype (Fig. 3J).

One of the key effector functions of macrophages is their ability to engulf and destroy cellular debris and foreign material [20], so we examined the phagocytic functional capacity of polarized macrophages. Representative flow-cytometry dot plots depicted in Fig. 3F reveal blunted phagocytosis of OVA-DQ by inflammatory RA macrophages compared with M0 and 'M2-like'. Further quantification indicates a significant decrease in the phagocytic capacity of RA inflammatory macrophage populations, relative to RA M0 and RA 'M2-like' (Fig. 2B, $P < 0.05$). Representative histograms indicate the shift from passive to active phagocytosis (Fig. 3F). These data suggest that the hyper-inflammatory profile of 'M1-like' RA macrophages results in a functional impairment in their

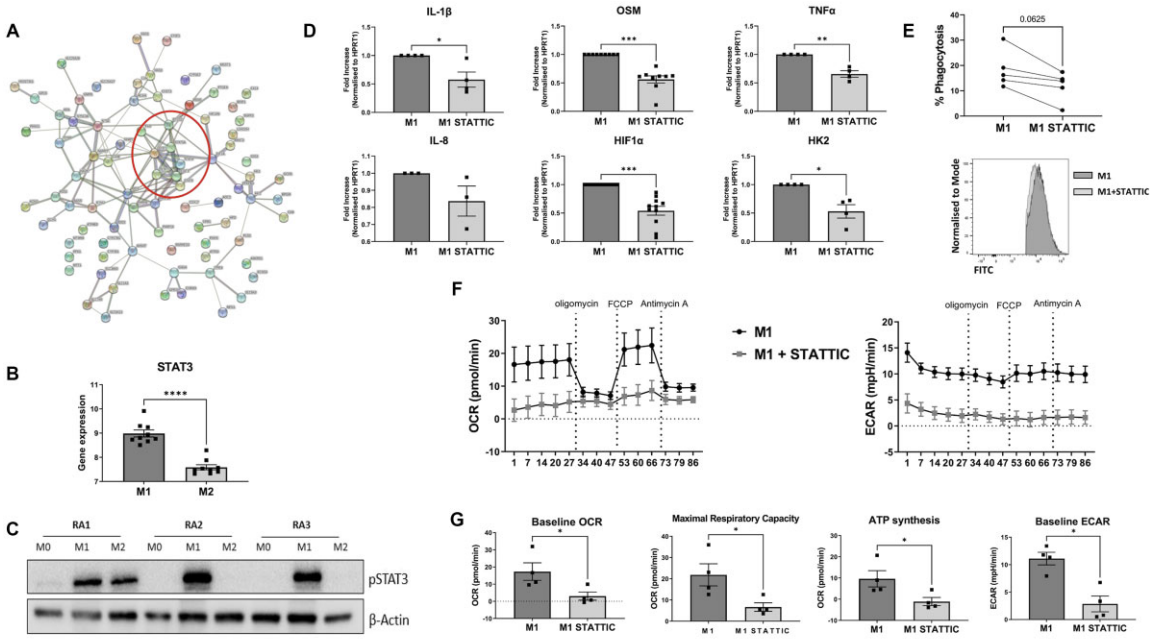

Figure 4. STAT3 regulation of macrophage phenotype. (**A**) STRING analysis of metabolism associated DEGs enriched in RA M1 *vs* M2. (**B**) Dot plot depicting *STAT3* gene expression in RA polarized monocyte-derived macrophages ($n = 9$). (**C**) Representative western blot demonstrating protein expression of pSTAT3 and β-actin control for M0, M1 and M2 macrophages from three independent RA patients. (**D**) Dot plots representing inflammatory and metabolic gene expression of RA M1 macrophages ± STATTIC ($n = 4$–11). (**E**) Line graphs and representative histogram representing phagocytic activity of RA M1 macrophages ± STATTIC ($n = 5$). (**F**) Average Seahorse bioenergetic profiles demonstrating OCR and ECAR of RA M1 macrophages ± STATTIC RA ($n = 4$). (**G**) Dot plots representing baseline OCR, ECAR, maximal respiratory capacity and ATP synthesis of RA M1 macrophages ± STATTIC RA ($n = 4$). Data expressed as mean (S.E.M.) using Wilcoxon signed rank and paired *t*-test; $^*P < 0.05$ significantly different. DEGs: differentially expressed genes; OCR: oxygen consumption rate; ECAR: extracellular acidification rate

ability to phagocytose. Indeed, failure to clear cellular debris may stimulate other infiltrating immune cells and thus perpetuate the inflammatory response further [21].

Distinct RA macrophage phenotype is STAT3 dependent

Given the key role of cellular metabolism in shaping myeloid cell phenotype and function we decided to focus on DEGs with a significant role in cellular bioenergetics. Selecting metabolism-associated genes that were significantly enriched in RA inflammatory macrophages, predicted interactions using STRING analysis are depicted in Fig. 4A. The resulting pathway diagram allows the homing in on central hubs. Interestingly, many molecules of the JAK/STAT signalling pathway are clustered at the epicentre of this diagram.

This was of significant interest as the JAK/STAT pathway was one of the top enriched pathways in RA 'M1-like' macrophages compared with 'M2-like' in the IPA analysis (Fig. 3D and E). Specifically, within this pathway, STAT3 signalling was observed to be enriched in RA inflammatory macrophages (Fig. 3D and E) and is one of the central nodes of the STRING analysis (Fig. 4A). Gene expression indicates that RA inflammatory macrophages have significantly elevated *STAT3* expression (Fig. 4B, $P < 0.05$). This was also confirmed at the protein level (Fig. 4C), suggesting that STAT3 signalling is associated with macrophage inflammatory function in RA.

Moreover, inhibition of STAT3 using the selective inhibitor STATTIC resulted in significant decreased expression of pro-inflammatory mediators (Fig. 4D, $P < 0.05$), with minimal effect on cell viability as demonstrated by annexin/PI apoptosis and crystal violet assays (Supplementary Fig. S2, available at *Rheumatology* online). Representative flow cytometry plots clearly depict the minimal effect of STATTIC on cell viability when compared with vehicle control (75% *vs* 80.7% live cells) as observed by annexin V/PI expression (Supplementary Fig. S2A, available at *Rheumatology* online). No significant effect of STATTIC was observed for *SOCS3* gene expression (Supplementary Fig. S3A, available at *Rheumatology* online.) STAT3 inhibition, however, fails to restore phagocytic function in inflammatory macrophages; instead STATTIC decreases RA inflammatory macrophage phagocytic function further (Fig. 4E). In addition, STAT3 inhibition significantly dampened expression of *HIF1α*, the master regulator of cellular bioenergetics, as well as the glycolytic enzyme *HK2* in inflammatory RA macrophages (Fig. 4D, $P < 0.05$). In parallel, average energy profiles are depicted in Fig. 4F and demonstrate that STAT3 inhibition results in downregulation in both oxidative phosphorylation and glycolysis, along with significant decreases in baseline glycolysis, mitochondrial respiration, maximal respiratory capacity and ATP synthesis (Fig. 4G, $P < 0.05$).

Novel role for metabolic enzyme NAMPT in driving RA macrophage phenotype

Analysis of the DEGs between RA 'M1-like' and 'M2-like' macrophages also identified *NAMPT* and several other genes involved in NAD^+ metabolism (such as *IDO1/2*, *NNMT* and *KYNU*) as central molecules in polarization of inflammatory RA macrophages (Fig. 5A and B). NAMPT is a rate-limiting enzyme in the NAD^+ salvage pathway and has been implicated in RA pathogenesis [22–24].

NAMPT inhibition resulted in significant abrogation of pro-inflammatory mediators (Fig. 5C, $P < 0.05$) and

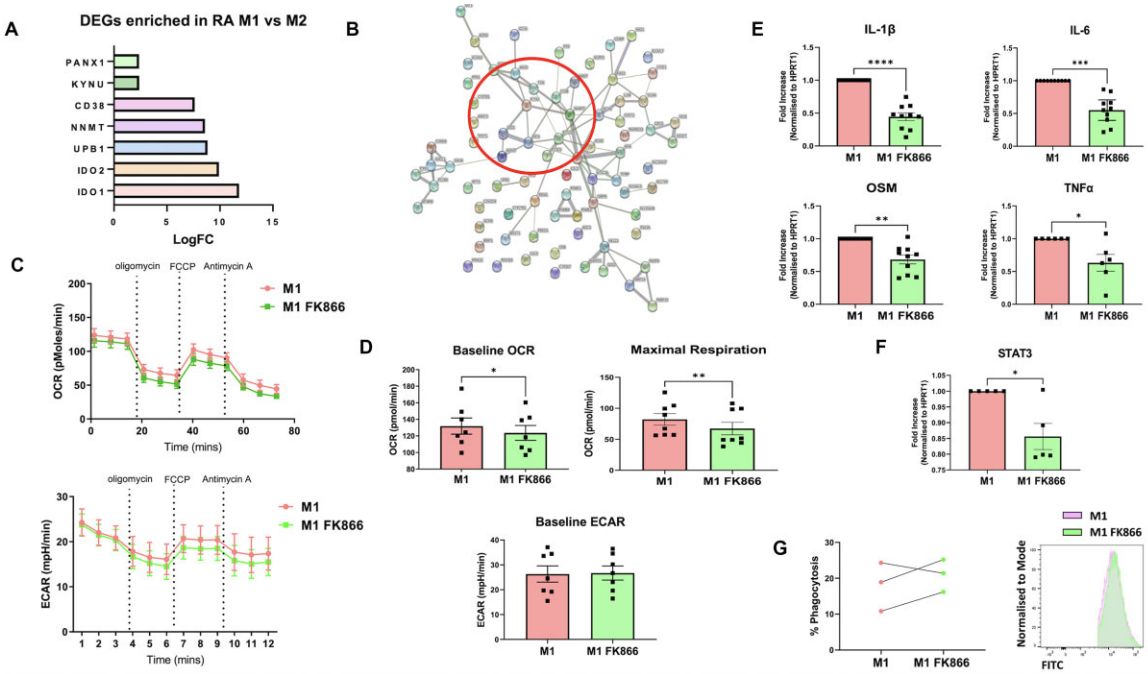

Figure 5. Novel role for NAMPT in directing macrophage inflammatory phenotype. (**A**) Bar chart depicting NAD^+ metabolism associated DEGs enriched in RA M1 *vs* M2. (**B**) STRING analysis of DEGs enriched in RA M1 *vs* M2. (**C**) Average Seahorse bioenergetic profiles demonstrating OCR and ECAR of RA M1 macrophages ± FK866 ($n = 8$). (**D**) Dot plots representing baseline OCR, ECAR and maximal respiratory capacity of RA M1 macrophages ± FK866 ($n = 8$). (**E**) Dot plots representing inflammatory gene expression of RA M1 macrophages ± FK866 ($n = 6$–10). (**F**) Dot plot representing STAT3 gene expression in RA inflammatory macrophages ± FK866 ($n = 6$). (**G**) Line graphs and representative histogram representing phagocytic activity of RA inflammatory macrophages ± FK866 ($n = 3$). Data expressed as mean (S.E.M.) using Wilcoxon signed rank and paired *t*-test; $^*P < 0.05$ significantly different. DEGs: differentially expressed genes

reciprocal inhibition of *STAT3* gene expression and activation (Fig. 5D, $P < 0.05$, Supplementary Fig. S3B, available at *Rheumatology* online), suggesting interplay between these two key signalling pathways. Finally, the reduced phagocytic phenotype of RA inflammatory macrophages is partially reversed upon NAMPT inhibition (Fig. 5E), with no effect on cell viability as demonstrated by annexin/PI apoptosis and crystal violet assays (Supplementary Fig. S2, available at *Rheumatology* online). Representative flow cytometry plots indicate 80.7% live cells (annexin V/PI expression; Q4) in DMSO vehicle control *vs* 77.7% live cells in FK866-treated cells, indicating little to no effect of NAMPT inhibition on macrophage viability (Supplementary Fig. S2A, available at *Rheumatology* online).

Discussion

Macrophages are a heterogeneous family of immune cells, critically involved in directing the immune response in RA. They are remarkably plastic which allows them to assume a classically activated, pro-inflammatory 'M1-like' state or an alternatively activated, immunoregulatory 'M2-like' state, two distinct poles of a wide macrophage activation state spectrum. Deciphering the mechanisms underpinning macrophage polarized phenotype may provide insights into the signalling pathways that contribute to the imbalance of inflammatory macrophages that has been reported in RA pathogenesis.

In this study we demonstrate that RA monocyte-derived macrophages are poised to produce pro-inflammatory mediators and retain a memory bias from their circulating monocyte precursors towards inflammation. The induction of pro-inflammatory mechanisms is coupled with altered mitochondrial morphology and enhancement of both oxidative phosphorylation and glycolysis in RA compared with HC. Further analysis of polarized RA macrophages revealed striking differences in inflammatory, bioenergetic and phagocytic function. Transcriptomic differences revealed specific enrichment of members of the JAK-STAT signalling pathway, particularly STAT3, in addition to enrichment of many members of the NAD salvage pathway, particularly NAMPT in RA pro-inflammatory macrophages. Using specific inhibitors for both STAT3 (STATTIC) and NAMPT (FK866) resulted in inhibition of the hyperinflammatory phenotype observed in these RA macrophages, and reciprocal interplay between these two signalling pathways. Finally, the observed decreased phagocytic function of pro-inflammatory RA macrophages was reversed upon NAMPT inhibition.

Consistent with previous studies [25–28] we demonstrate that the intermediate subpopulation ($CD14^+CD16^+$) of circulating monocytes is significantly increased in RA compared with HC, which are associated with a pro-inflammatory function [25–28]. Gene expression analysis revealed that RA monocytes are primed for inflammation and display hyper-inflammatory gene signatures, consistent with our recent study [18]. Interestingly, however, RA monocyte-derived macrophages maintain the hyper-inflammatory memory bias of their precursor cells, with significantly higher expression of pro-inflammatory cytokines compared with HC. This is in line with studies examining monocytes/macrophages in coronary artery disease suggesting that monocytes are preprogramed for inflammation and subsequent differentiation into pro-inflammatory macrophages [29]. Interestingly, monocyte priming appears to be disease specific, with studies indicating that circulating monocytes from GCA patients display inflammatory signatures similar to HC [30].

Recent evidence has demonstrated the importance of metabolic rewiring in guiding the functional phenotype of macrophages [31]. In this study we demonstrate that RA macrophages are highly energetic and display a state of heightened mitochondrial activity compared with HC, thus indicating they are already metabolically primed once they enter the synovial space. We also demonstrate significant increased expression of key metabolic genes, *PFKFB3*, *HK2* and *HIF1α*, in RA macrophages compared with healthy ones. Although we have not investigated this at the protein level, our previous study in RA circulating monocytes confirms significant protein upregulation of these key glycolytic enzymes in RA monocytes compared with healthy ones [18]. This was further reflected in the ultrastructure analysis of RA macrophage mitochondria which exhibit a dominance of elongated, dense mitochondria compared with healthy macrophages, consistent with studies reporting remodelling of mitochondria-associated membranes in RA and coronary artery disease macrophages to enhance mitochondrial activity [32].

This link between metabolic plasticity and inflammation in RA is not surprising. Many studies report a bioenergetic crisis within the inflamed synovium, highlighting the role of altered cellular bioenergetics in driving RA pathogenesis [25, 33–36]. Previous studies have shown that succinate-mediated stabilization of HIF1α results in IL-1β secretion and reactive oxygen species production from macrophages [26, 27], while GPR91-deficient mice display reduced macrophage activation and IL-1β production [28]. Studies have also demonstrated that deletion of HIF1α in myeloid cells of CIA mice results in decreased macrophage infiltration and joint swelling due to reduced macrophage mobility and invasive capacity [37]. Additionally, silencing of the amino acid transporter, SLC7A5, results in a significant decrease of IL-1β and glycolysis in RA monocytes and macrophages [38].

In this study we also demonstrate significant functional impairment in the phagocytic ability of M1 macrophages compared with M0 and M2 macrophages. Delayed or reduced phagocytosis has previously been observed in RA mononuclear phagocytes, leading to an increase in reactive oxygen species generation and resulting in subsequent prioritization of chemotactic behaviour and cytokine release over phagocytosis [39]. In the context of RA, the failure of M1-polarized macrophages to efficiently clear cellular debris, coupled with their observed hyper-inflammatory phenotype, may further stimulate the infiltration of other immune cells into the synovium, thus propagating the inflammatory response [21].

This study identified a key role for the transcription factor STAT3 in influencing RA macrophage polarization. STAT3 also mediates inflammatory and metabolic effects in RA monocytes, indicating that this mechanism occurs early in macrophage differentiation [18]. Previous studies have shown that activation of STAT3 is associated with *in vivo* synovial hypoxia in RA, while hypoxia-induced STAT3 activation causes upregulation of HIF1α [40, 41]. Furthermore, inhibition of JAK-STAT signalling switches the metabolic and inflammatory profile of synovial cells, including monocytes away from pathogenic mechanisms and towards resolution of inflammation [18, 42]. Furthermore, we and others have demonstrated bidirectional interactions between STAT3 and key glycolytic enzymes HIF1α, PKM2 and HK2 as well as glycolysis itself [18, 29, 40, 41, 43]. In addition, we demonstrate that STAT3 inhibition fails to restore the phagocytic activity of inflammatory RA macrophages. This is in line with previous studies demonstrating that macrophage pSTAT3 is a prophagocytic mediator via a STAT3–IL-10–IL-6 feedback loop to allow macrophages to maintain their scavenging functions [44, 45].

Finally, this study highlights the role of the novel metabolic target NAMPT, with pharmacological inhibition of NAMPT leading to a decrease in the pro-inflammatory profile in RA macrophages. Previous studies have shown elevated expression of NAMPT in the synovial tissue, SF and serum of RA patients [24, 46–48] This is in line with studies demonstrating that FK866 results in deceased RA disease severity and joint inflammatory cytokine secretion [49], and reduced inflammatory mediator expression in RA monocytes indicating that NAMPT plays a key role early in the life cycle of macrophages. Interestingly NAMPT inhibition also results in significantly reduced *STAT3* gene expression, thus linking these two key signalling pathways.

In summary, we demonstrate that RA monocyte-derived macrophages are imprinted with disease-specific hyper-inflammatory and hyper-metabolic signatures, and retain this functional commitment, such that mature macrophages conserve this phenotype and results in impaired phagocytic ability, indicating that monocytes are capable of building immunological memory via epigenetic imprinting [50]. Finally, our data suggest that targeting of NAMPT and/or STAT3 could a promote resolution of chronic inflammation observed in RA driven by the myeloid compartment.

Supplementary data

Supplementary data are available at *Rheumatology* online.

Data availability

The data underlying this article are available in the article and in its online supplementary material. RNA sequencing data are available in a public, open access repository. All raw and processed files for each sample are deposited on national center for biotechnology information (NCBI), ascension number GSE223325 https://www.ncbi.nlm.nih.gov/geo/query/acc.cgi?acc=GSE223325 and are publicly available without any restrictions of their subsequent use.

Funding

This work was supported by the Irish Research Council (GOIPG/2016/1567 to M.M.H.), Science Foundation Ireland (SFI 20/FFP-P/8666), Centre for Arthritis and Rheumatic Diseases, and Arthritis Ireland.

Disclosure statement: Q.S. and S.N. are current or former employees of Janssen Research & Development, Johnson & Johnson. The remaining authors have declared no conflicts of interest.

Acknowledgements

M.M.H. designed and performed experiments, analysed data and wrote the manuscript. U.F. designed experiments, analysed data and wrote the manuscript. T.Mc.G. designed, performed experiments and analysed data. V.M. performed experiments and analysed data. S.A. performed experiments and analysed data. Q.S. performed RNA-seq data analysis. S.N. analysed data. D.J.V. recruited patients and obtained patient samples, analysed data and wrote the manuscript.

References

1. Brennan FM, McInnes IB. Evidence that cytokines play a role in rheumatoid arthritis. J Clin Invest 2008;118:3537–45.
2. McInnes IB, Schett G. The pathogenesis of rheumatoid arthritis. N Engl J Med 2011;365:2205–19.
3. Szekanecz Z, Koch AE. Mechanisms of disease: angiogenesis in inflammatory diseases. Nat Clin Pract Rheumatol 2007;3:635–43.
4. Drexler SK, Kong PL, Wales J, Foxwell BM. Cell signalling in macrophages, the principal innate immune effector cells of rheumatoid arthritis. Arthritis Res Ther 2008;10:216.
5. Ng CT, Biniecka M, Kennedy A *et al.* Synovial tissue hypoxia and inflammation in vivo. Ann Rheum Dis 2010;69:1389–95.
6. Kennedy A, Ng CT, Chang TC *et al.* Tumor necrosis factor blocking therapy alters joint inflammation and hypoxia. Arthritis Rheum 2011;63:923–32.
7. Harty LC, Biniecka M, O'Sullivan J *et al.* Mitochondrial mutagenesis correlates with the local inflammatory environment in arthritis. Ann Rheum Dis 2012;71:582–8.
8. Kennedy A, Ng CT, Chang TC *et al.* Tumor necrosis factor blocking therapy alters joint inflammation and hypoxia. Arthritis Rheum 2011;63:923–32.
9. Mulherin D, Fitzgerald O, Bresnihan B. Synovial tissue macrophage populations and articular damage in rheumatoid arthritis. Arthritis Rheum 1996;39:115–24.
10. Bresnihan B, Pontifex E, Thurlings RM *et al.* Synovial tissue sublining CD68 expression is a biomarker of therapeutic response in rheumatoid arthritis clinical trials: consistency across centers. J Rheumatol 2009;36:1800–2.
11. Tak PP, Smeets TJ, Daha MR *et al.* Analysis of the synovial cell infiltrate in early rheumatoid synovial tissue in relation to local disease activity. Arthritis Rheum 1997;40:217–25.
12. Merad M, Manz MG, Karsunky H *et al.* Langerhans cells renew in the skin throughout life under steady-state conditions. Nat Immunol 2002;3:1135–41.
13. Udalova IA, Mantovani A, Feldmann M. Macrophage heterogeneity in the context of rheumatoid arthritis. Nat Rev Rheumatol 2016;12:472–85.
14. Möttönen M, Isomäki P, Saario R *et al.* Interleukin-10 inhibits the capacity of synovial macrophages to function as antigen-presenting cells. Br J Rheumatol 1998;37:1207–14.
15. Palacios BS, Estrada-Capetillo L, Izquierdo E *et al.* Macrophages from the synovium of active rheumatoid arthritis exhibit an activin a-dependent pro-inflammatory profile. J Pathol 2015;235:515–26.
16. Biniecka M, Fox E, Gao W *et al.* Hypoxia induces mitochondrial mutagenesis and dysfunction in inflammatory arthritis. Arthritis Rheum 2011;63:2172–82.
17. Saha S, Shalova IN, Biswas SK. Metabolic regulation of macrophage phenotype and function. Immunol Rev 2017;280:102–11.
18. McGarry T, Hanlon MM, Marzaioli V *et al.* Rheumatoid arthritis CD14+ monocytes display metabolic and inflammatory dysfunction, a phenotype that precedes clinical manifestation of disease. Clin Transl Immunol 2021;10:e1237.
19. Aletaha D, Neogi T, Silman AJ *et al.* 2010 Rheumatoid arthritis classification criteria: an American College of Rheumatology/European League Against Rheumatism collaborative initiative. Arthritis Rheum 2010;62:2569–81.
20. Hirayama D, Nakase H. Molecular sciences the phagocytic function of macrophage-enforcing innate immunity and tissue homeostasis. 2017. www.mdpi.com/journal/ijms (14 January 2020, date last accessed).
21. Gierut A, Perlman H, Pope RM. Innate immunity and rheumatoid arthritis. Rheum Dis Clin North Am 2010;36:271–96.
22. Franco-Trepat E, Alonso-Pérez A, Guillán-Fresco M *et al.* Visfatin as a therapeutic target for rheumatoid arthritis. Expert Opin Ther Targets 2019;23:607–18.
23. Šenolt L, Krytůfková O, Hulejová H *et al.* The level of serum visfatin (PBEF) is associated with total number of B cells in patients with rheumatoid arthritis and decreases following B cell depletion therapy. Cytokine 2011;55:116–21.
24. Matsui H, Tsutsumi A, Sugihara M *et al.* Visfatin (pre-B cell colony-enhancing factor) gene expression in patients with rheumatoid arthritis. Ann Rheum Dis 2008;67:571–2.
25. Biniecka M, Canavan M, McGarry T *et al.* Dysregulated bioenergetics: a key regulator of joint inflammation. Ann Rheum Dis 2016;75:2192–200.
26. Tannahill GM, Curtis AM, Adamik J *et al.* Succinate is an inflammatory signal that induces IL-1β through HIF-1α. Nature 2013;496:238–42.
27. Mills EL, Kelly B, Logan A *et al.* Succinate dehydrogenase supports metabolic repurposing of mitochondria to drive inflammatory macrophages. Cell 2016;167:457–70.e13.
28. Littlewood-Evans A, Sarret S, Apfel V *et al.* GPR91 senses extracellular succinate released from inflammatory macrophages and exacerbates rheumatoid arthritis. J Exp Med 2016;213:1655–62.
29. Shirai T, Nazarewicz RR, Wallis BB *et al.* The glycolytic enzyme PKM2 bridges metabolic and inflammatory dysfunction in coronary artery disease. J Exp Med 2016;213:337–54.
30. Watanabe R, Hilhorst M, Zhang H *et al.* Glucose metabolism controls disease-specific signatures of macrophage effector functions. JCI Insight 2018;3:e123047.
31. Van den Bossche J, O'Neill LA, Menon D. Macrophage immunometabolism: where are we (going)? Trends Immunol 2017;38:395–406.
32. Zeisbrich M, Yanes RE, Zhang H *et al.* Hypermetabolic macrophages in rheumatoid arthritis and coronary artery disease due to glycogen synthase kinase 3b inactivation. Ann Rheum Dis 2018;77:1053–62.
33. Hanlon MM, Canavan M, Barker BE, Fearon U. Metabolites as drivers and targets in rheumatoid arthritis. Clin Exp Immunol 2022;208:167–80.
34. Fearon U, Hanlon MM, Floudas A, Veale DJ. Cellular metabolic adaptations in rheumatoid arthritis and their therapeutic implications. Nat Rev Rheumatol 2022;18:398–414.
35. McGarry T, Biniecka M, Veale DJ, Fearon U. Hypoxia, oxidative stress and inflammation. Free Radic Biol Med 2018;125:15–24.
36. Fearon U, Canavan M, Biniecka M, Veale DJ. Hypoxia, mitochondrial dysfunction and synovial invasiveness in rheumatoid arthritis. Nat Rev Rheumatol 2016;12:385–97.
37. Cramer T, Yamanishi Y, Clausen BE *et al.* HIF-1α is essential for myeloid cell-mediated inflammation. Cell 2003;112:645–57.
38. Yoon BR, Oh Y-J, Kang SW, Lee EB, Lee W-W. Role of SLC7A5 in metabolic reprogramming of human monocyte/macrophage immune responses. Front Immunol 2018;9:53.
39. Arleevskaya MI, Gabdoulkhakova AG, Filina JV, Zabotin AI, Tsibulkin AP. Mononuclear phagocytes in rheumatoid arthritis patients and their relatives - family similarity. Open Rheumatol J 2011;5:36–44.
40. Jung JE, Lee HG, Cho IH *et al.* STAT3 is a potential modulator of HIF-1-mediated VEGF expression in human renal carcinoma cells. FASEB J 2005;19:1296–8.
41. Gao W, McCormick J, Connolly M *et al.* Hypoxia and STAT3 signalling interactions regulate pro-inflammatory pathways in rheumatoid arthritis. Ann Rheum Dis 2015;74:1275–83.
42. McGarry T, Orr C, Wade S *et al.* JAK/STAT blockade alters synovial bioenergetics, mitochondrial function, and proinflammatory mediators in rheumatoid arthritis. Arthritis Rheumatol 2018;70:1959–70.
43. Li M, Jin R, Wang W *et al.* STAT3 regulates glycolysis via targeting hexokinase 2 in hepatocellular carcinoma cells. Oncotarget 2017;8:24777–84.
44. Campana L, Starkey Lewis PJ, Pellicoro A *et al.* The STAT3-IL10-IL6 pathway is a novel regulator of macrophage efferocytosis and phenotypic conversion in sterile liver injury. J Immunol 2018;200:1169–87.
45. Tigerprints T, Tisch L. Comparing the anti-inflammatory properties of STATTIC to indirubin-E804 in RAW264.7 macrophages.

2021. https://tigerprints.clemson.edu/all_theses/3504 (10 October 2022, date last accessed).
46. Nowell MA, Richards PJ, Fielding CA *et al.* Regulation of pre–B cell colony-enhancing factor by STAT-3–dependent interleukin-6 trans-signaling: implications in the pathogenesis of rheumatoid arthritis. Arthritis Rheum 2006;54:2084–95.
47. Gómez R, Conde J, Scotece M *et al.* What's new in our understanding of the role of adipokines in rheumatic diseases? Nat Rev Rheumatol 2011;7:528–36.
48. Abella V, Scotece M, Conde J *et al.* Adipokines, metabolic syndrome and rheumatic diseases. J Immunol Res 2014;2014:343746.
49. Busso N, Karababa M, Nobile M *et al.* Pharmacological inhibition of nicotinamide phosphoribosyltransferase/visfatin enzymatic activity identifies a new inflammatory pathway linked to NAD. PLoS One 2008;3:e2267.
50. Neele AE, Van Den Bossche J, Hoeksema MA, De Winther MPJ. Epigenetic pathways in macrophages emerge as novel targets in atherosclerosis. Eur J Pharmacol 2015;763:79–89.